

Formation of GaN Nanorods in Monodisperse Spherical Mesoporous Silica Particles

E. Yu. Stovpiaga^{a,*}, D. A. Kurdyukov^a, D. A. Kirilenko^a, and V. G. Golubev^a

^a Ioffe Institute, St. Petersburg, 194021 Russia

*e-mail: kattrof@gvg.ioffe.ru

Received March 3, 2020; revised March 10, 2020; accepted March 10, 2020

Abstract—Gallium-nitride nanorods with a diameter of 15–40 nm and length of 50–150 nm are synthesized in monodisperse spherical mesoporous silica particles (MSMSPs) by high-temperature annealing of the Ga₂O₃ precursor in ammonia. The template material (*a*-SiO₂) is selectively removed by etching the composite MSMSP/GaN particles with HF to give individual GaN nanorods. It is shown that the size of the GaN nanorods substantially exceeds the pore size of the MSMSPs (diameter ~3 nm, length ~10 nm). A possible mechanism by which GaN nanorods are formed is proposed. Redistribution of the material within the composite MSMSP/GaN particles possibly occurs via the surface diffusion of gaseous molecules within mesopores and via the diffusion of Ga and N atoms in *a*-SiO₂.

Keywords: GaN, mesoporous silica, nanorods, template synthesis

DOI: 10.1134/S106378262007012X

1. INTRODUCTION

Great interest has continued in recent decades in obtaining and studying semiconductor materials of varied morphology because these materials possess electrical, transport, mechanical, and optical properties different from those in the bulk material [1, 2]. In particular, GaN nanorods are promising for various fields of micro-, nano-, and optoelectronics and nanophotonics [3, 4]. The rod-like shape of the crystals is characteristic of GaN, and their growth in the direction of the hexagonal axis *c* is faster than that along the *a* and *b* axes [5, 6]. GaN nanorods can be obtained by various methods: vapor-phase epitaxy [7, 8], laser ablation [9, 10], molecular-beam epitaxy [11, 12], plasma-chemical vapor deposition [3], etc. There exist various mechanisms for the formation and growth of GaN nanorods, which depend on their synthesis method and process parameters [14, 15].

One way to obtain GaN nanocrystals is via synthesis of the material within cylindrical mesopores of silicas of the types MCM-41 [16] and SBA-15 [17]. The spatial hindrance to growing crystallites of various shapes is determined by the diameter and length of mesopores and also by the size and shape of the template particles. For example, GaN nanoparticles with sizes of several nanometers (~3 nm) are formed in pores in the case of MCM-41 [18] and 7 × 50 nm nanorods in the case of SBA-15 [17]. Despite active studies of the mechanisms by which gallium-nitride

crystals grow, there is hardly any published evidence about the mechanisms by which nanoscale forms of GaN are formed in porous matrices.

A particular place among porous silicas is occupied by monodisperse spherical mesoporous silica particles (MSMSPs) having an internal system of cylindrical nanochannels of the same diameter (3 nm) with a volume that accounts for 60% of the particle volume [19–21]. We have obtained on the basis of MSMSPs nanocomposite particles containing oxides [22], metals [23], semiconductor materials [24], and carbon nanodots [25]. When the substances are synthesized, chemical and physical processes occur similarly in monodisperse particles of the same shape with identical pore structures. Therefore, MSMSPs are ideally suitable as a model object (nanoreactor) for studying the growth mechanisms of anisotropic crystals in a silica matrix.

Here, we discuss the possible mechanism by which GaN nanorods are formed in MSMSPs in the course of high-temperature heterogeneous synthesis from gas- and solid-phase precursors. The GaN nanorods being formed have a size that substantially exceeds that of mesopores in the template. The growth of coarse GaN nanorods via the disappearance of fine nanorods is probably due to a decrease in the total energy and occurs via the diffusion of gallium atoms and Ga₂O molecules within MSMSPs. Morphological and structural analyses of the materials obtained are made.

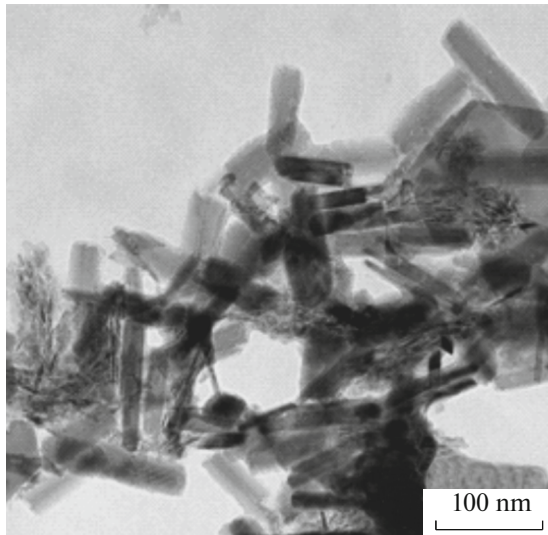
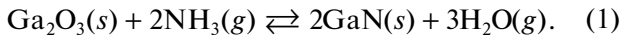


Fig. 1. TEM image of GaN nanorods.

2. EXPERIMENTAL

Nanocomposite MSMSP/GaN particles were synthesized by the procedure described in [26]. MSMSPs having a diameter of 210 ± 20 nm and cylindrical pores with a diameter of 3.1 ± 0.2 nm and a length of 10–15 nm [19–21, 27] were filled with melt of the crystal hydrate $\text{Ga}(\text{NO}_3)_3 \cdot 8\text{H}_2\text{O}$. The samples were dried at a temperature of 400 K and then annealed at $T = 800$ K for 3 h for the nitrate to decompose into Ga_2O_3 . The mesopores were filled with Ga_2O_3 to 40 vol % of the pore volume [26]. The subsequent annealing of MSMSPs filled with gallium oxide was performed in an atmosphere of ammonia (1 bar) at a temperature of 1300 K for 20 h in order to obtain gallium nitride within the particles:



To etch the template material (*a*- SiO_2), a weighed portion of nanocomposite MSMSP/GaN particles was placed in a hydrofluoric acid solution (40 wt % HF) for 2 h. Then, the undissolved material (filler substance) was separated by centrifugation, followed by washing with deionized water, and ultrasonically redispersed.

Microscopic studies were carried out by transmission electron microscopy (TEM) on a Jeol JEM-2100 microscope (Japan). A X-ray fluorescence microanalysis (XFMA) was performed with an Oxford Instruments INCA energy-dispersive X-ray spectrometer built into the electron microscope. The particle size distribution was determined by the dynamic light scattering (DLS) method on a Malvern Zetasizer Nano instrument at a temperature of 298 K. The Raman spectra were measured at room temperature on a Horiba Jobin Yvon T64000 spectrometer, with the second harmonic of a Nd:YAG laser ($\lambda = 532$ nm) serving as the source of light, at an excitation power on the sample surface not exceeding $P = 2$ kW/cm².

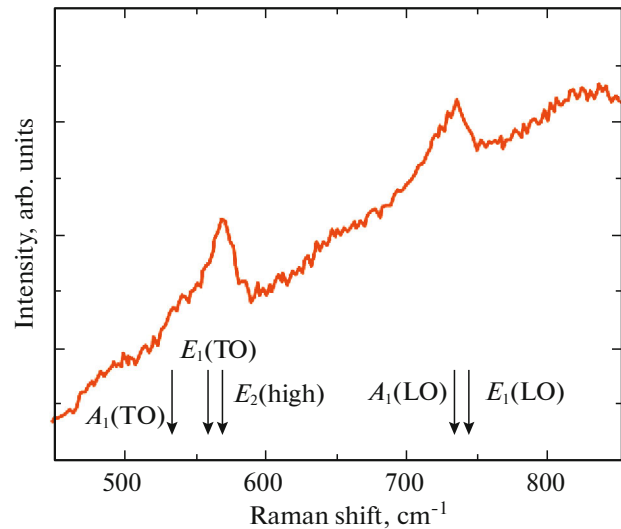


Fig. 2. Raman spectrum of GaN nanorods. The lines show the positions of the Raman-active phonon modes of hexagonal GaN.

3. RESULTS AND DISCUSSION

TEM analysis of the material obtained after dissolving the template material demonstrated that it has the form of nanorods with a diameter of 15 to 40 nm and a length of 50 to 150 nm (Fig. 1). According to Raman data (Fig. 2) the nanorods are composed of nanocrystalline hexagonal GaN [26, 28, 29]. According to the data furnished by atomic-force microscopy [26] and TEM (Fig. 3), there is no bulk gallium nitride on the surface of MSMSP/GaN composite particles. At the same time, the observed dimensions of the GaN nanorods substantially exceed the pore size in MSMSPs (diameter 3 nm, length 10–15 nm [19–21, 27]).

The size of objects observed in Fig. 1 is correlated with that of the coherent-scattering region in GaN (29 nm), determined by processing the X-ray diffraction pattern of the composite MSMSP/GaN particles by the Rietveld method [26]. In addition, inclusions several tens of nanometers in size, which contain, according to XFMA, gallium atoms, are observed in high-resolution TEM (HRTEM) images of the composite particles (Fig. 3). According to DLS data, the average hydrodynamic size of the GaN nanorods is 160 ± 25 nm (Fig. 4), which is in agreement with the TEM data (Fig. 1 and inset of Fig. 4). It can be stated on the basis of the above data that the nanorods were formed within MSMSPs during the high-temperature heterogeneous synthesis of GaN from the Ga_2O_3 precursor introduced into the mesopores. After the template is removed, the GaN nanorods are dispersed in an aqueous dispersion medium.

Let us consider in detail the possible mechanism by which GaN crystallites are formed and grow within the MSMSPs. We assume that particles with an average diameter of ~ 3 nm are first formed within the mesopores, as shown previously for the example of carbon

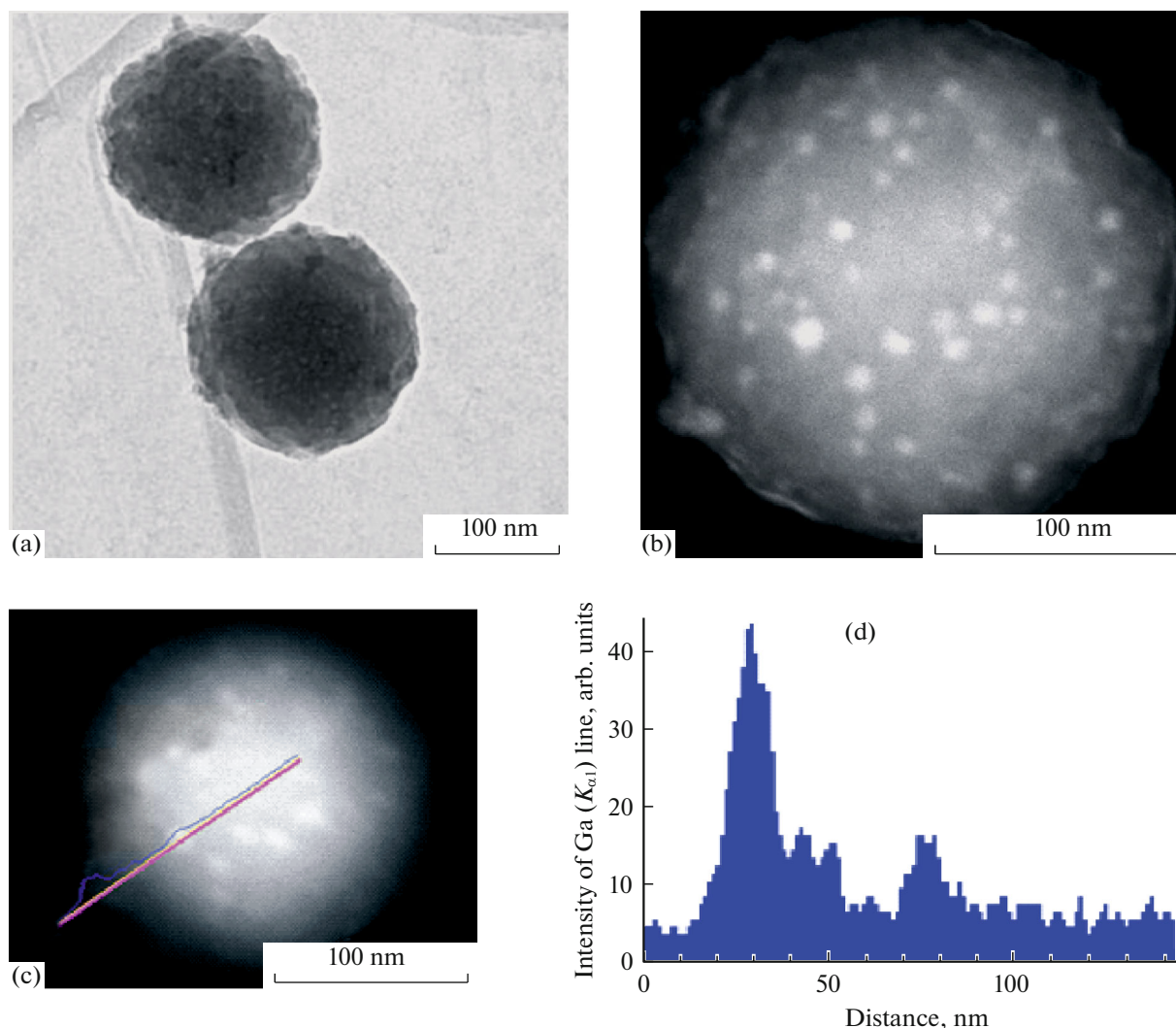


Fig. 3. (a) TEM and (b, c) HRTEM images of MSMSP/GaN nanocomposite particles; (d) gallium distribution profile obtained by the XFMA method from a single particle.

nanodots [25]. The smaller the size of a particle, the higher its surface energy per unit volume and the higher the chemical potential. The difference $\Delta\mu$ between the chemical potentials of GaN particles with different sizes favors a mass transfer from fine to coarse particles. The main reason for the mass transfer is that the system tends to decrease its surface energy due to a decrease in the number of small particles, and there occurs a transition to an energetically more favorable state. Lowering of the total energy of the system with increasing size of the nanorods and a decrease in their μ is a thermodynamically favorable process [30, 31], described by the Gibbs–Thompson formula [32]:

$$\Delta\mu = \mu_r - \mu_\infty = \frac{2\sigma_{\text{GaN-SiO}_2} V_{\text{GaN}}}{3r}.$$

Here, μ_r and μ_∞ are the chemical potentials of the component in a nanoparticle of radius r and in a particle with infinite size, respectively; $\sigma_{\text{GaN-SiO}_2}$ is the

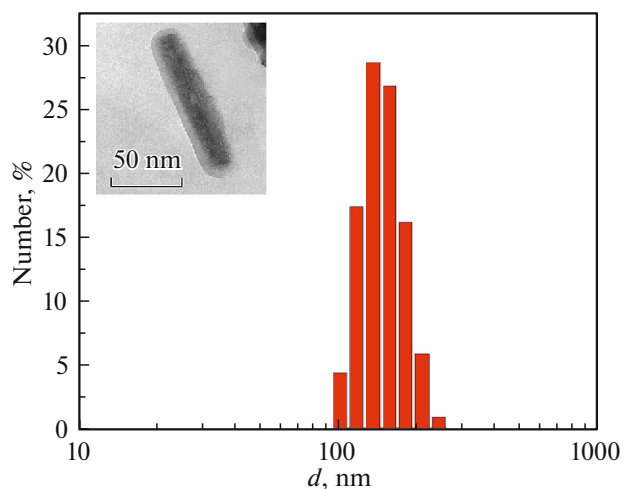


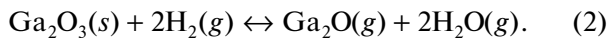
Fig. 4. GaN-nanorod size distribution measured by the DLS method. The inset shows the magnified TEM image of a GaN nanorod.

surface tension at the GaN–SiO₂ interface; and V_{GaN} is the molar volume of GaN.

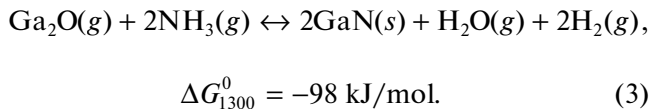
Within the pores of the MSMSPs, there occurs, in the presence of nanorods with even a narrow size scatter, mass transfer of the substance from fine nanorods (to the point of their complete disappearance) to coarser nanorods. This process will occur until the rate at which fine nanorods disappear becomes insignificant and the mass-transfer rate is negligible (the system will approach the thermodynamically equilibrium state).

Two ways of substance transfer are possible within MSMSPs. First, molecules of gaseous components may move within the mesopores of MSMSPs via surface diffusion. Second, amorphous silica forming the MSMSPs is gradually softened at a synthesis temperature of 1300 K, the porous structure within the particles disappears, and, therefore, the diffusion of Ga and N atoms within amorphous silica becomes the main mass-transfer pathway.

Let us consider the mass transfer of a substance through the gas phase. The thermal decomposition of ammonia (pressure 1 bar) yields, according to the reaction $2\text{NH}_3 = \text{N}_2 + 3\text{H}_2$, hydrogen (equilibrium pressure of H₂ at the synthesis temperature is hundreds of millibars [33, 34]), which reacts with gallium oxide [35, 36]:



The calculated Gibbs energy of reaction (2), $\Delta G_{1300}^0 = +95$ kJ/mol, which corresponds to the equilibrium constant $K_p = p_{\text{H}_2\text{O}}^2 p_{\text{Ga}_2\text{O}} / p_{\text{H}_2}^2 = 10^{-4}$. At a hydrogen pressure of 100 mbar, the equilibrium pressure of the product formed in reaction (2), Ga₂O, is 10 mbar, i.e., reaction (2) indeed can occur within pores of silica particles during the synthesis of GaN. Previously a similar process of the conversion of Ga₂O₃ to Ga₂O was observed in [35, 37]. Presumably, Ga₂O is transferred within mesopores to subsequently give gallium nitride [35, 36], in accordance with the following reaction equation:



Reactions (2) and (3) are responsible for the mass transfer and for the coarsening of GaN nanorods. The formation of gaseous Ga at a temperature of 1300 K is unlikely because of its low vapor pressure (10⁻⁷ bar) [38]. Therefore, Ga(g) is not involved in mass transfer and is not considered here. We believe that GaN nanocrystallites with a diameter of up to 3 nm and varied length can be formed in the given stage within three-nanometer MSMSP pores.

Together with the formation of GaN from Ga₂O₃, the already formed GaN nanoparticles or nanorods may be partly converted to Ga₂O via the inverse reaction (3). Ga₂O is transferred and reacts with NH₃ (present in the system in an excess amount) to give GaN (3) near the surface of coarser GaN nanorods, thereby making these even larger. Similar gas-transport reactions [forward and reverse reactions (3)] are characteristic of binary compounds of various compositions [39]. The water vapor formed in the course of the reaction in which GaN is synthesized from Ga₂O₃ (1) serve as a transport agent.

At a temperature of 1300 K, porous silica is softened [40]. The pores in MSMSPs are closed and the subsequent mass transfer of the substance occurs via the diffusion of Ga and N atoms within SiO₂. GaN formed in the preceding stage is transferred to coarser nanorods and this occurs, in accordance with the Gibbs–Thompson equation, until rods comparable in size with the MSMSPs themselves are formed. At a temperature of 1300 K, the diffusion coefficients of Ga and N atoms in SiO₂ are $D(\text{Ga}) = 5 \times 10^{-11}$ cm²/s [41, 42] and $D(\text{N}) = 1.4 \times 10^{-4}$ cm²/s [43], respectively. Therefore, the growth rate of GaN nanorods in MSMSPs will be primarily determined by the diffusion rate of Ga atoms. This rate, calculated by the formula $v \approx \sqrt{(D(\text{Ga})\tau)}$, where τ is the diffusion time (in s), was found to be 550 nm in 1 min, which allows Ga atoms to move within the whole spherical particle, thereby providing the growth of GaN nanorods. Together with the diffusion of Ga and N atoms in SiO₂, there occurs the diffusion of Si and O atoms in GaN [44]. These processes lead to redistribution of the material within the MSMSPs.

4. CONCLUSIONS

It was demonstrated in the study that the heterogeneous synthesis of GaN from Ga₂O₃ under thermodynamically equilibrium conditions via annealing at a temperature of 1300 K in an atmosphere of ammonia yields gallium-nitride nanorods within MSMSPs. The size of GaN nanorods differs from the initial size of the mesopores (3.1 nm). According to TEM data, their diameter varies from 15 to 40 nm, and their size, from 50 to 150 nm. According to the Raman data, the nanorods are composed of hexagonal GaN.

A possible mechanism by which GaN nanorods are formed was suggested. This mechanism is based on two kinds of mass transfer of the substance within MSMSPs: (i) transfer of molecules of gaseous components via surface diffusion and (ii) substance transfer via the diffusion of Ga and N atoms within amorphous SiO₂. The growth of GaN nanorods is energetically favorable, and, presumably, coarse GaN nanorods are

formed via the absorption (disappearance) of fine GaN crystallites in MSMSPs.

ACKNOWLEDGMENTS

We are grateful to A.N. Smirnov for Raman measurements of the GaN nanorods.

Measurements by transmission electron microscopy were performed on equipment of the federal Collective Use Center “Materials science and diagnostics in advanced technologies” (Ioffe Institute).

FUNDING

The study was financed by the State budget under State assignment no. 0040-2019-0012.

CONFLICT OF INTEREST

The authors state that they have no conflict of interest.

REFERENCES

1. C.-C. Tsai, G.-H. Li, Y.-T. Lin, C.-W. Chang, P. Wadekar, Q. Y.-S. Chen, L. Rigutti, M. Tchernycheva, F. H. Julien, and L.-W. Tu, *Nanoscale Res. Lett.* **6**, 631 (2011).
2. D. Bimberg, *Semiconductor Nanostructures* (Springer, Berlin, Heidelberg, 2008).
3. R. Agarwal and C. M. Lieber, *Appl. Phys. A* **85**, 209 (2006).
4. C. M. Lieber and Z. L. Wang, *MRS Bull.* **32**, 99 (2007).
5. D. Ehretraut, E. Meissner, and M. Bockowski, *Technology of Gallium Nitride Crystal Growth* (Springer, Berlin, Heidelberg, 2010).
6. K. Kishino, H. Sekiguchi, and A. Kikuchi, *J. Cryst. Growth* **311**, 2063 (2009).
7. X. L. Chen, J. Y. Li, Y. G. Cao, Y. Lan, H. Li, M. He, C. Wang, Z. Zhang, and Z. Qiao, *Adv. Mater.* **12**, 1432 (2000).
8. J. C. Johnson, H. J. Choi, K. P. Knutsen, R. D. Schaller, P. Yang, and R. J. Saykally, *Nat. Mater.* **1**, 106 (2002).
9. X. F. Duan and C. M. Lieber, *J. Am. Chem. Soc.* **122**, 188 (2000).
10. D. K. T. Ng, L. S. Tan, and M. H. Hong, *Curr. Appl. Phys.* **6**, 403 (2006).
11. K. A. Bertness, A. Roshko, L. M. Mansfield, T. E. Harvey, and N. A. Sanford, *J. Cryst. Growth* **300**, 94 (2007).
12. M. Tchernycheva, C. Sartel, G. Cirlin, L. Travers, G. Patriarche, J.-C. Harmand, L. S. Dang, J. Renard, B. Gayral, L. Nevou, and F. Julien, *Nanotechnology* **18**, 385306 (2007).
13. J.-W. Jao, Y.-F. Zhang, Y.-H. Li, C. Su, X.-M. Song, H. Yan, and R.-Z. Wang, *Sci. Rep.* **5**, 17692 (2015).
14. G. Suo, S. Jiang, J. Zhang, J. Li, and M. He, *Adv. Condens. Matter Phys.* **2014**, 456163 (2014).
15. A. N. Semenov, D. V. Nechaev, S. I. Troshkov, A. V. Nashchekin, P. N. Brunkov, V. N. Jmerik, and S. V. Ivanov, *Semiconductors* **52**, 1770 (2018).
16. H. Parala, A. Devi, W. Rogge, A. Birkner, and R. A. Fischer, *J. Phys. IV (France)* **11**, 473 (2001).
17. C. T. Yang and M. H. Huang, *J. Phys. Chem. B* **109**, 17842 (2005).
18. K. Dimos, L. Jankovi, I. B. Koutselas, M. A. Karakasides, R. Zboril, and P. Komadel, *J. Phys. Chem. C* **116**, 1185 (2012).
19. E. Yu. Trofimova, D. A. Kurdyukov, Yu. A. Kukushkina, M. A. Yagovkina, and V. G. Golubev, *Glass Phys. Chem.* **37**, 378 (2011).
20. E. Yu. Trofimova, D. A. Kurdyukov, S. A. Yakovlev, D. A. Kirilenko, Yu. A. Kukushkina, A. V. Nashchekin, A. A. Sitnikova, M. A. Yagovkina, and V. G. Golubev, *Nanotechnology* **24**, 155601 (2013).
21. E. Yu. Stovpiaga, D. A. Kurdyukov, Yu. A. Kukushkina, V. V. Sokolov, and M. A. Yagovkina, *Glass Phys. Chem.* **41**, 316 (2015).
22. E. Yu. Stovpiaga, D. A. Eurov, D. A. Kurdyukov, A. N. Smirnov, M. A. Yagovkina, V. Yu. Grigorev, V. V. Romanov, D. R. Yakovlev, and V. G. Golubev, *Phys. Solid State* **59**, 1623 (2017).
23. D. A. Kurdyukov, D. A. Eurov, E. Yu. Stovpiaga, S. A. Yakovlev, D. A. Kirilenko, and V. G. Golubev, *Phys. Solid State* **56**, 1033 (2014).
24. D. A. Kurdyukov, N. A. Feoktistov, D. A. Kirilenko, A. N. Smirnov, V. Yu. Davydov, and V. G. Golubev, *Semiconductors* **53**, 1048 (2019).
25. D. A. Kurdyukov, D. A. Eurov, E. Yu. Stovpiaga, D. A. Kirilenko, S. V. Konyakhin, A. V. Shvidchenko, and V. G. Golubev, *Phys. Solid State* **58**, 2545 (2016).
26. E. Yu. Stovpiaga, D. A. Eurov, D. A. Kurdyukov, A. N. Smirnov, M. A. Yagovkina, D. R. Yakovlev, and V. G. Golubev, *Semiconductors* **52**, 1123 (2018).
27. D. A. Kurdyukov, D. A. Eurov, D. A. Kirilenko, J. A. Kukushkina, V. V. Sokolov, M. A. Yagovkina, and V. G. Golubev, *Microporous Mesoporous Mater.* **223**, 225 (2016).
28. V. Yu. Davydov, Yu. E. Kitaev, I. N. Goncharuk, A. N. Smirnov, J. Graul, O. Semchinova, D. Uffmann, M. B. Smirnov, A. P. Mirgorodsky, and R. A. Evarestov, *Phys. Rev. B* **58**, 12899 (1998).
29. V. Yu. Davydov, R. E. Dunin-Borkovski, V. G. Golubev, J. L. Hutchison, N. F. Kartenko, D. A. Kurdyukov, A. B. Pevtsov, N. V. Sharenkova, J. Sloan, and L. M. Sorokin, *Semicond. Sci. Technol.* **16**, L5 (2001).
30. N. K. Thanh, N. Maclean, and S. Mahiddine, *Chem. Rev.* **114**, 7610 (2014).
31. S. I. Sadovnikov and A. I. Gusev, *Phys. Solid State* **60**, 1308 (2018).
32. Yu. M. Petrov, *Clusters and Small Particles* (Nauka, Moscow, 1986) [in Russian].

33. A. F. White and W. Mellvill, *J. Am. Chem. Soc.* **27**, 373 (1905).
34. D. Dirtu, L. Odochian, A. Pui, and I. Humelnicu, *Centr. Eur. J. Chem.* **4**, 666 (2006).
35. H. Kiyono, T. Sakai, M. Takahashi, and S. Shimada, *J. Cryst. Growth* **312**, 2823 (2010).
36. K. Kachel, M. Korytov, D. Gogova, Z. Galazka, M. Albrecht, R. Zwierz, D. Siche, S. Golka, A. Kwasniewski, M. Schmidbauer, and R. Fornari, *Cryst. Eng. Commun.* **14**, 8536 (2012).
37. D.-H. Kuo and W.-H. Wu, *J. Electrochem. Soc.* **156**, K1 (2009).
38. R. Fornanini, *Single Crystals of Electronic Materials* (Woodhead, Elsevier, 2018).
39. H. Schäffer, *Chemical Transport Reactions* (Elsevier, Amsterdam, 1964).
40. G. M. Gajiev, D. A. Kurdyukov, and V. V. Travnikov, *Nanotechnology* **17**, 5349 (2006).
41. A. H. van Ommen, *J. Appl. Phys.* **57**, 15 (1985).
42. A. S. Grove, O. Lkistiko, Jr. Sah, and C. T. Sah, *J. Phys. Chem. Solids* **25**, 985 (1964).
43. J. Kioseoglou, M. Katsikini, K. Termentzidis, I. Karakostas, and E. C. Paloura, *J. Appl. Phys.* **121**, 054301 (2017).
44. R. Jakiela, A. Barcz, E. Dumiszewska, and A. Jagoda, *Phys. Status Solidi C* **3**, 1416 (2006).

Translated by M. Tagirdzhanov